THEORETICAL AND EXPERIMENTAL INVESTIGATIONS OF A PROPELLER WORKING AT STATIC CONDITION

Iwasaki, Matsunosuke
Department of Aeronautical Engineering, Kyushu University : Professor

SASAKI, Ryohei
Faculty of Engineering, Kyushu University

SHIKI, Tomohisa
Department of Aeronautical Engineering, Kyushu University

HIMORI, Atsumu
Department of Aeronautical Engineering, Kyushu University

https://doi.org/10.5109/7167118

出版情報：Reports of Research Institute for Applied Mechanics. 16 (52), pp.33-67, 1968. 九州大学応用力学研究所
バージョン：
権利関係：

Reports of Research Institute for Applied Mechanics
Vol. XVI, No. 52, 1968

THEORETICAL AND EXPERIMENTAL INVESTIGATIONS OF A PROPELLER WORKING AT STATIC CONDITION†

by Matsunosuke IWASAKI*, Ryohei SASAKI**, Tomohisa SHIKI***
and Atsumu HIMORI****

Summary

Formulae to calculate the static performance of a propeller are derived assuming infinite number of blades. The distributions of section lift coefficient, thrust coefficient grading, power coefficient grading etc. along radius of that four-bladed propeller are obtained without successive approximation, which is set at three kinds of blade angle of 4.35°, 9.35° and 14.35°. The effect of section drag coefficient and tangential induced velocity on the above distributions is discussed. It is found that the drag affects the power coefficient grading and that the tangential induced velocity, inspite of its small absolute value, has considerable effect on the blade element characteristics of inner radius. The experimental results with a model propeller having the same principal items show considerably good agreement with the theoretical values in the range of thirty per cent to fifty-five percent of outer radius. Theoretical thrust and power coefficients agree with the experimental ones within the error of ten per cent which are measured with a load cell and a torque meter.

Introduction

There have been many papers on the calculation of static propeller performance since the beginning of the year of 1960.[1] And now some decisive conclusions and methods seem to be obtained by Ordway, Borst, etc.[2),3)]. Therefore it seems that the necessity to write more about the solution of the problem of the propeller at static state decreases. Precise inspection of these papers, however, shows that some ambiguity is found in the fundamental theoretical consideration

† Presented at the anual meeting of the Japan Society for Aeronautical and Space Science, April 5, 1967, in Tokyo.

* Professor, Department of Aeronautical Engineering, Kyushu University, Hakozaki, Fukuoka City, Japan: Member (additional post) of Research Institute for Applied Mechanics, Kyushu University.

** Engaged in the present research when he was a reaearch student of Faculty of Engineering, Kyushu University.

*** Performed the research, when he was the fourth year student of undergraduate course, Dept. Aero. Engr. Kyushu Univ.

**** Made the research one year later than Shiki, when he was the fourth year student of undergraduate course, Dept. Aero. Engr., Kyushu Univ.

of the flow around a propeller and the results of experiment. For example, the measured inflow velocity distribution along blades is considerably different from the calculated one in the case of reference 2, while the calculated thrust coefficient C_T, power coefficient C_P and the Figure of Merit F. M. at static state agree well with the results of experiments. Then it might be said that these good agreement of the thrust coefficient etc. were due to the integral procedure by which individual errors in thrust coefficient grading $dC_T/d(r_0/R)$ and power coefficient grading $dC_P/d(r_0/R)$ are cancelled, so that the values of C_T, C_P and F. M. close to the true ones are obtained. This is the first expample of ambiguities concerning the problem of a propeller of static working state. Now let us see another aspect which may be acceptable as the subject of consideration. Gartshore[4] published an interesting paper in which he calculated static thrust distribution along a blade assuming that the helical vortices are spilled from the radial point of $0.9R$. His results of calculation for C_T, C_P etc. do not show good agreement with experiment, but the form of distribution curves of $dC_T/d(r_0/R)$, $dC_P/d(r_0/R)$ and inflow velocity is very much instructive. On the other hand Adams[5] describes, according to his experimental observation, that the blade element near tips works as the one of a windmill which results in large thrust coefficient grading and negative power coefficient grading. This fact seems to have been explained by Gartshore's theory. The authors are not yet sure whether this wihdmill state is covered by the theory of Ordway etc., and think that the configulation near the tip can now be interpreted in various ways so that the accurate informations at its static state have not been yet obtained. These slight inspections of the present state of investigations of propellers of static working condition indicate that there[6),7] are many problems which are not yet settled and remain unsolved. Now let us see the problems which the authors treat in the present paper. By reading the paper of Ordway, Borst etc.[1),2),3] the authors found that they considered the influence of the form, including the pitch of the helical vortex sheets, of slipstream on the working state of propellers of static condition to be very large. The authors thought, however, that the flow state near the tips of propellers would not have so much effect on the distributions of $dC_T/d(r_0/R)$ and $dC_P/d(r_0/R)$ at comparatively inner radial points ranging presumably from 0.2 of radius ratio of r_0/R to 0.7 or 0.8. Therefore we tried to calculate the performance of a propeller at its static working state by a vortex theory of infinite number of blades[6),7] taking only the effect of pitch angle of helical votices into consideration. The reason why the authors took the effect of pitch angle into consideration is that according to the experience of one of the authors,[7] among many factors only this has the most predominant effect on the induced velocity on the propeller disc. On taking the effect of pitch angle into consideration, the authors did not apply any elaborate treatments or considerations, but used the pitch angle at propeller disc. The reason for this is as follows:

As shown by Lock's[8], Iwasaki's[9] and Kawada's[10] investigations, the pitch angle on the propeller plane seems to be the most suitable pitch angle of helical vortices for the propeller performance calcularion. Taking the factors of deformation of slipstream into consideration, this selection of pitch angle may show satisfactory result.[7]

The present apparently rough treatment of the working state of a propeller at static state, at first sight, may be thought to result in an unrealistic results for the blade element near the tip of propeller, because investigators of propellers know that the effect of the configulation of strong tip helical vortices has predominant effect on these blade elements. It was expected, however, that for the blade elements located at relatively inner side of propeller radius, the present results of calculation might agree with experimental results because of their long distance from tips. Theoretical approach which was performed above was compared with the authors' experiments of a model four-bladed propeller, and the distributions of thrust and power coefficients grading over the range of radius ratio from $r_0/R=0.3$ to $r_0/R=0.75$ agreed with each other within the accuracy of ten per cent. As stated before, in the authors' theory the assumption of infinite number of blades is included, so that the agreement over this region will not be expected. These results might make some contribution to the researches of a propeller of static working state. Even only the fact that the distributions of $dC_T/d(r_0/R)$ from $r_0/R=0.3$ to 0.75 show good agreement with experiments may be useful for the investigation of static thrust, because then the investigation of static thrust can be concentrated to the one for the range of 0.75 $\sim$1.0. In the following the method, the experimental results etc. of the present investigations will be described.

§ 1 FUNDAMENTAL FORMULAE

The induced velocity by a propeller, which has infinite number of blades, is given by[7]

$$\frac{\boldsymbol{v}}{V}=\int_{0\ or\ root}^{1.0\ or\ tip} d\gamma \sum_{i=1}^{\infty}\left(\frac{R}{r_{1i}}V_{ri}\cot\phi_{1i}\right)\cdot\boldsymbol{i}+\left[\int_{root}^{tip} d\gamma\sum_{i=1}^{\infty}\frac{R}{r_{1i}}\left(V_{ti}-\frac{\omega_{zi}}{\omega_{xi}}V_{ri}\right)-\right.$$

$$\left.-d\gamma_0\frac{\pi}{\left(\frac{r}{R}\right)}\left[1+\frac{z}{\left\{\left(\frac{r}{R}\right)^2+\left(\frac{z}{R}\right)^2\right\}^{1/2}}\right]-\int_{root}^{tip}\gamma\cdot\left(\frac{R}{r_0}\right)^2 U_{rz/R=0}\, d\left(\frac{r_0}{R}\right)\right]\boldsymbol{j}+$$

$$+\int_{root}^{tip} d\gamma\cdot\sum_{i=1}^{\infty}\left(\frac{R}{r_{1i}}V_{zi}\cot\phi_{1i}\right)\cdot\boldsymbol{k} \tag{1-1}$$

where

- $\boldsymbol{v}$: induced velocity vector, v_r or v_x radial, v_t or v_y tangential, and v_z axial
- V: velocity of oncoming flow
- γ : nondimensional representation of circulation around blade element at radius r_0(0 indicates propeller plane), $\gamma=B\Gamma/4\pi^2RV$, B is number of blades, R is outer radius of a propeller, in this report instead of γ, $\gamma'=B\Gamma/4\pi^2R^2\Omega=\gamma\cdot V/\Omega R$ is used.
- r_1 : radius of cylindrical vortex sheet at z which is spilled from r_{01} (see Fig. 1-1)

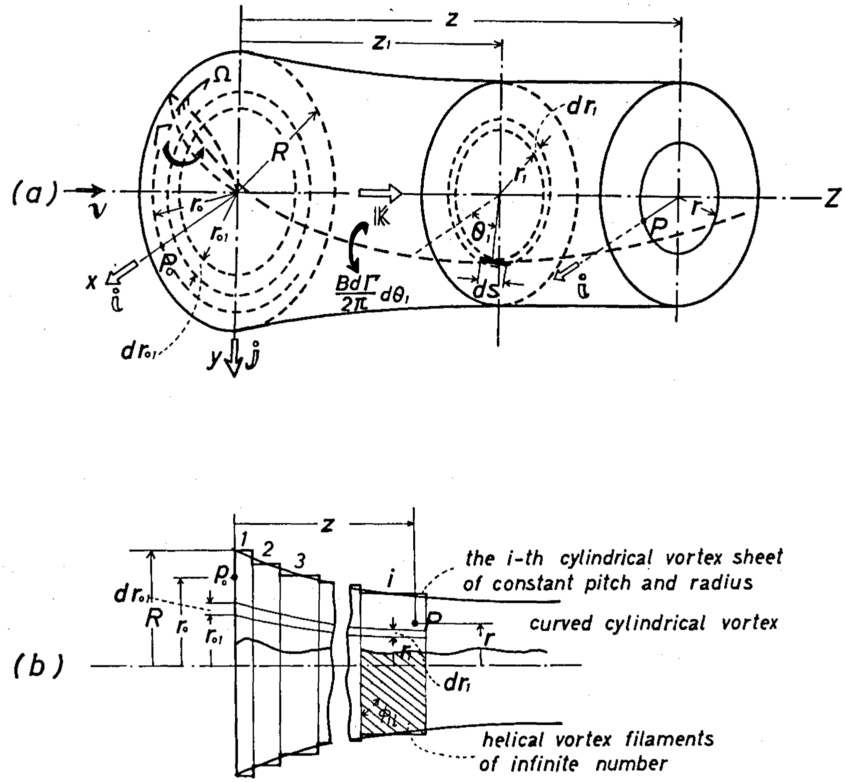

Fig. 1-1 (a) Propeller disc and its slipstream full of helical vortex filaments (on the assumption of infinite number of blades)
(b) Approximation of curved cylindrical vortex by vortex cylinder of constant radius and pitch having finite axial lengh

i: subscript which respresents the i-th cylindrical vortex sheet which has constant radius r.

$\mathbf{i}$, $\mathbf{j}$, $\mathbf{k}$: unit vector along x, y and z directions. At P, $\mathbf{i}$ is radial, $\mathbf{j}$ tangential and $\mathbf{k}$ axial directions.

$d\gamma_0$: the strength of circulation of straight vortex filament shed from a boss

x, y, z: orthogonal coordinates of point P, where x: radial y: tangential z: axial

ω_x, ω_y, ω_z: radial, tangential axial components of the element of vortex filaments at (r_1, θ_1, z_1) of cylindrical coordinates, $\cot \phi_{1i} = (\omega_y/\omega_z)_i$

V_r: radial induction factor at the point $P(r/r_1, z/r_1)$ by the cylindrical vortex sheet of radius r_1, which extends from $z=0$ to $z=$infinity

V_t: tangential induction factor at point P by the cylindrical vortex sheet stated above

V_z: axial induction factor at P by the same cylindrical vortex sheet
R: outer radius of propeller.

In the following description the subscript $_o$ means the values on the propeller disc, and the subscript $_1$ shows the values corresponding to the trailing helical vortices. For example $_{01}$ means the values concerning the trailing helical vortices on the propeller disc.

In Eq. (1.1-1) the symbol of summation means, as shown in the lower figure of Fig. 1-1, the summation of the effects from the cylindrical vortex of different radius and of finite length. These various cylinders represent approximately the continuous vortex cylinders with smoothly curved generation lines.

At radius r_{01} cylindrical vortex sheet of nondimensionalized strength $d\gamma = d\gamma/d(r_0/R)\cdot d(r_0/R)$ is spinned. This forms the smooth vortex cylinder stated above.

Now we shall neglect the radial component $v_r/\Omega R$ of Eq. (1-1), because the radial spanwise component on the propeller disc has no substantial effect on the effective angle of attack of blade elements, and because, as stated in Introduction, the deformation of vortex cylinder by V_r seems to have little effect on the distribution curves of $dC_T/d(r_0/R)$ and $dC_P/d(r_0/R)$ over the radial region of $\gamma_0/R = 0.3 \sim 0.75$. The main purpose of the present reseach is to obtain the information over this range, without any hope for any information of the region near tip. Thus this simplification may be justified. By the neglection of $v_r/\Omega R$ the stepwise cylindrical vortex cylinders become circular cylinders of constant radii so that the procedure of summation disappears, and V_{ri}, V_{ti} and V_{zi} which represent the induction factors for the i-th vortex cylinder become V_r, V_t and V_z respectively. These correspond to semi-infinite vortex cylinder ranging from the propeller disc to downstream infinity. The $\boldsymbol{i}$ component of induced velocity of course disappears by the neglection of radial component. The $\boldsymbol{j}$ component or the tangential induced velocity is affected by the terms

$$\text{(a)} \int_{root}^{tip} d\gamma \sum_{i=1}^{\infty}\left(\frac{R}{r_{1i}}\cdot V_{ti}\right), \quad \text{(b)} -\int_{root}^{tip} d\gamma \frac{R}{r_{1i}}\cdot \sum_{i=1}^{\infty}\frac{\omega_{zi}}{\omega_{xi}} V_{ri},$$

$$\text{(c)} -d\gamma_0 \frac{\pi}{\left(\frac{r}{R}\right)}\left[1+\frac{z/R}{\left\{\left(\frac{r}{R}\right)^2+\left(\frac{z}{R}\right)^2\right\}^{1/2}}\right] \text{ and } \text{(d)} -\int_0^1 \gamma\left(\frac{R}{r_0}\right)^2 U_{rz/R=0}\cdot d\left(\frac{r_0}{R}\right)$$

The term (a) is the induced velocity by the cylindrical vorex sheets over which infinite number of helical vortex filamants are wrapped. The term (b) is due to the vortex sheet elements of radial direction. The term (c) is the contribution of central vortex filament of nondimensionalized strength $d\gamma_0$ spilled from a boss. And the term of (d) is the effect of bound vortex, or in the present case of infinite number of blabes, the circular vortex disc on the propeller plane.

The term (b), of course, is neglected. The term (c) is contained in (a) in the present paper, and the term (d) need not be considered in the present investigation, because the bound vortex disc itself does not induce the induced velocity at the propeller plane where the vortex disc is located. Then the $\boldsymbol{j}$ component is represented only by the term (a). The $\boldsymbol{k}$ component is the induced velocity of the axial direction of a propeller which is induced by vortex cylinders over which infinite number of helical vortex filaments are wrapped. cot ϕ_{ti} is the cotangent of average pitch angle of helical vortex filaments over the i-th vortex cylinder. In the present case, the authors adopted the value of ϕ_{01} on the propeller plane, because, as described in Introduction, this value seems to be most suitable for the calculation of propeller performances. As generally known, at low advance ratio the predominant induced velocity is the $\boldsymbol{k}$ component. In the present case of static working state the advance ratio also is zero. Therefore it can be said that this $\boldsymbol{k}$ component is the most important one in Eq.(1-1). After the consideration stated above, Eq. (1-1) is reduced to a simple form of

$$\frac{\boldsymbol{v}}{V}=\boldsymbol{j}\int_{root}^{tip} d\gamma\cdot\frac{R}{r_{01}}V_t+\boldsymbol{k}\cdot\int_{root}^{tip} d\gamma\cdot\frac{R}{r_{01}}V_z\cot\phi_{01} \tag{1-2}$$

Applying this formula to our present case, we must make $\boldsymbol{v}$ nondimensional by some other reference speed, because V is zero at atatic working state of a propeller. As the nondimensionalizing factor ΩR may be appropriate for the present case, where Ω is angular velocity of a propeller. Then, multiplying both sides of Eq. (1.1-2) by $\frac{V}{\Omega R}$, this equation is written as

$$\frac{\boldsymbol{v}}{\Omega R}=\boldsymbol{j}\cdot\frac{v_t}{\Omega R}+\boldsymbol{k}\cdot\frac{v_z}{\Omega R}=\boldsymbol{j}\cdot\int_{root}^{tip} d\gamma_0'\cdot\frac{R}{r_{01}}V_t+\boldsymbol{k}\int_{root}^{tip} V_z\frac{R}{r_{01}}(\cot\phi_{01}\,d\gamma_0') \tag{1-3}$$

where $\gamma_0'=\frac{B\Gamma}{4\pi^2R^2\Omega}$ and ϕ_{01} is the average pitch angle of helical vortex filaments over the cylindrical vortex sheets of radius r_{01}. This value, stated previously, is assumed to be constant from the propeller disc to far downstream infinity, and throughout the following calculation it is identified with the value on the propeller plane. $d\gamma_0'$ is the nondimensionalized strength of vortex spinned at radius r_{01}/R on the propeller plane. This is all the strength of vortices from blade elements of B per unit angular space around the axis of rotation of a propeller. In the present theory, by the assumption of infinite number of blades, the discrete B helical vortices spinned out of the blade elements is reduced to homogeneous vortex cylinder having its mean radius of r_{01}/R, and $d\gamma_0'$ above described corresponds, therefore, to the total strength of curved vortex sheet contained in the one radian circular arc of this vortex cylinder.

Now we shall consider the value of V_t and V_z. As shown in Iwasaki's paper,[7] for the semi-infinite vortex cylinder over which vortex filaments are wrapped and which extends from the plane of a pepeller to far downstream infinity, the values of V_t and V_z is as follows:

$$\begin{aligned}
&\text{(a)}\quad V_z=0 \quad \text{for} \quad r_0/R\big/r_{01}/R>1, \quad z/R=0 \text{ (or on plane of propeller)}\\
&\text{(b)}\quad V_z=-\frac{\pi}{2} \qquad r_0/R\big/r_{01}/R=1, \quad z/R=0 \qquad\qquad (1\text{-}4)\\
&\text{(c)}\quad V_z=-\pi \qquad r_0/R\big/r_{01}/R<1, \quad z/R=0
\end{aligned}$$

In other words, the cylindrical vortex sheets of radius r_{01}/R or r_1/R (now we are considering a cylinder of constant radius) induce axial induced velocity $d(v_{z0}/\Omega R)$ at radius r_0/R which is located inside r_{01}/R and on the propeller disc, but that vortex sheet does not induce axial induced volocity at the point on the propeller disc, situated outside the cylindrical vortex sheet, and at the point on the propeller disc, which is on the cylindrical vortex sheet it induces half amount of axial induced velocity or $\frac{1}{2}d(v_{z0}/\Omega R)$. Now let us see the property of V_t.

According to Iwasaki,[7)]

$$\begin{aligned}
&\text{(a)}\quad V_t=-\pi\cdot\left(\frac{r_{01}}{r_0}\right) \text{for} \quad r_0/R\big/r_{01}/R>1, \quad z/R=0\\
&\text{(b)}\quad V_t=-\frac{\pi}{2} \qquad r_0/R\big/r_{01}/R=1, \quad z/R=0 \qquad\qquad (1\text{-}5)\\
&\text{(c)}\quad V_t=0 \qquad r_0/R\big/r_{01}/R>1, \quad z/R=0
\end{aligned}$$

These mean that the tangential induced velocity is affected only by the vortex cylinders inside the radius r_0/R, and on the vortex cylinder it has half of the value just outside the vortex cylinder.

Next we shall find the relation between a blade element and its section lift coefficient etc. This is given by

$$r_0'=\left(\frac{ks}{2}\right)\left(\frac{r_0}{R}\right)\sqrt{\left(\frac{v_{z0}}{\Omega R}\right)^2+\left(\frac{r_0}{R}+\frac{v_{t0}}{\Omega R}\right)^2}\cdot\left\{\frac{\beta^\circ+|\alpha_0|^\circ}{57.29578^\circ}-\frac{1}{52.29578^\circ}\arctan\frac{v_{z0}/\Omega R}{r_0/R+v_{t0}/\Omega R}\right\} \qquad (1\text{-}6)$$

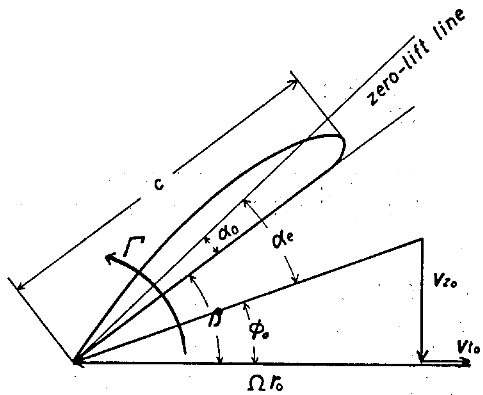

Fig. 1-2 Flow diagram of static condition at r_0

Flow diagram of blade element at radius r_0 at static working atate is shown in Fig. 1-2. The notations used in this figure have the following meanings;

$\alpha_0°$: Zero-lift angle measured from bottom flat surface or chord line of airfoil (in degrees), only for this notation the subscript zero means zerolift. It has negative sign.

$\beta°$: blade-angle at r_0, measured from the bottom flat surface or chord line of airfoil (in degrees)

$\phi_0°$: induced angle of attack of blade element at propeller disc.

$\alpha_e°$: effective angle of attack (in degrees)

c: chord length

Ω: angular velocity of propeller or $2n\pi$, where n is the number of rotations per second

c_l: section (two-dimensional) lift coefficient of blade element

$2\pi k$: $dc_l/d(\alpha_e°/57.29578°)$ or slope of lift curve of two-dimensional airfoil section

s: solidity, $Bc/2\pi r_0$.

γ_0': $B\Gamma/4\pi^2R^2\Omega$

subscript o means the values at propeller surface.

w_0: resultant inflow velocity to airfoil section or at propeller surface.

If we solve Eq. (1-6) with Eq. (1-3) considering the values of V_z and V_t according to Eqs. (1-4) and (1-5), the values of v_{z0}/R, v_{t0}/R, γ'_0 for r_0/R are obtained. Then the thrust coefficient C_T and the power coefficient C_P of a propeller are expressed as follows:

$$C_T=\frac{\text{Thrust}}{\rho n^3 D^4}=\int_{\left(\frac{r_0}{R}\right)_{root}}^{1,0}\frac{dC_T}{d\left(\frac{r_0}{R}\right)}d\left(\frac{r_0}{R}\right)=\left|-\pi^4\int_{\left(\frac{r_0}{R}\right)_{root}}^{1,0}\gamma_0'\left(\frac{r_0}{R}+\frac{v_{t0}}{\Omega R}\right)d\left(\frac{r_0}{R}\right)+\right.$$

$$\left.+\frac{\pi}{4}^3\int_{\left(\frac{r_0}{R}\right)_{root}}^{1,0}\left\{\left(\frac{v_{z0}}{\Omega R}\right)^2+\left(\frac{r_0}{R}+\frac{v_{t0}}{\Omega R}\right)^2\right\}\frac{r_0}{R}s\cdot c_d\sin\phi_0 d\left(\frac{r_0}{R}\right)\right| \qquad \text{(a)}$$

$$C_P=\frac{\text{Power}}{\rho n^2 D^5}=\int_{\left(\frac{r_0}{R}\right)_{root}}^{1,0}\frac{dC_P}{d\left(\frac{r_0}{R}\right)}d\left(\frac{r_0}{R}\right)=\pi^5\int_{\left(\frac{r_0}{R}\right)_{root}}^{1,0}\gamma_0'\left(\frac{v_{z0}}{\Omega R}\right)\left(\frac{r_0}{R}\right)d\left(\frac{r_0}{R}\right)+ \qquad \text{(1-7)}$$

where

$$+\frac{\pi}{4}^4\int_{\left(\frac{r_0}{R}\right)_{root}}^{1,0}\left\{\left(\frac{v_{z0}}{\Omega R}\right)^2+\left(\frac{r_0}{R}+\frac{v_{t0}}{\Omega R}\right)^2\right\}\left(\frac{r_0}{R}\right)^2 sc_d\cos\phi_0 d\left(\frac{r_0}{R}\right) \qquad \text{(b)}$$

C_T: thrust coefficient

C_P: power coefficient

ρ: air density

c_d: drag coefficient of two-dimensional airfoil section composing blade element.

$dG_T/d\left(\frac{r_0}{R}\right)$: thrust coefficient grading at r_0/R

$dC_P/d\left(\frac{r_0}{R}\right)$: power coefficient grading at r_0/R

In Eq. (1-7) (a) and (b) the former terms containing γ_0' represent the contribution of γ_0' around blade element and the latter terms including c_d is the contribution of drag coefficient c_d of the blade element to $dC_T/d\left(\frac{r_0}{R}\right)$ and $dC_P/d\left(\frac{r_0}{R}\right)$.

§2. PREPARATIONS FOR NUMERICAL CALCULATIONS

The numerical calculation is performed by approximating the distribution of circulation along blades by a stepwise distribution. The schematic figure of how to divide is shown in Fig. 2-1. The number of division n is usually more than

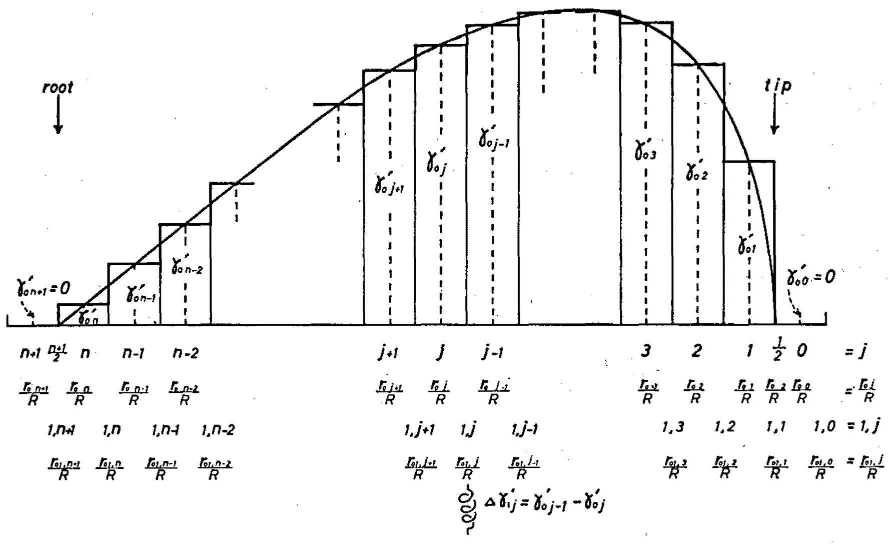

Fig. 2-1 Stepwise approximation of circulation

twenty-four for an electonic computer. The present calculation can be made also with a hand-operated calculation machine or a slide rule and an abacus. Then it may be more recommendable, than the present uniform n division, to take the division of

$\frac{r_0}{R}=0.1$, 0.3, 0.45, 0.55, 0.65, 0.75, 0.85, 0.925 and 0.975, or 0.05, 0.15, 0.25 0.35 0.45, 0.55 0.65, 0.75, 0.85, 0.925, and 0.975.

Taking Eqs. (1-4) and (1-5) into consideration this stepwise division reduces the expressions for $v_z/\Omega R$ and $v_t/\Omega R$ of Eq. (1-3) to very simple forms. Namely

$$\frac{v_{toj}}{\Omega R}=j \text{ component of } \frac{v}{\Omega R}=-\pi\frac{R}{r_{0j}}\sum_{k=n+1}^{j}\Delta\gamma'_k$$

$$=-\pi\frac{R}{r_{0j}}\{(\gamma_{0n}'-\gamma_0'_{n+1})+(\gamma_0'_{n-1}-\gamma_0'_n)+\cdots+(\gamma_0'_{j+1}-\gamma_0'_{j+2})+(\gamma_0'_j-\gamma_0'_{j+1})\}$$

$$=-\pi\frac{R}{r_{0j}}\gamma_0'_j+\pi\frac{R}{r_{0j}}\gamma_0'_{n+1}$$

where $\Delta\gamma'_{1k}=\gamma_0'_k-\gamma_0'_{k+1}$ (see Fig. 2-1).

As shown in Fig. 2-1 $\gamma_0'_{n+1}$ is equal to zero, so that this equation becomes

$$\frac{v_{toj}}{\Omega R}=-\pi\frac{R}{r_{0j}}\gamma_0'_j \tag{2-1}$$

On the other hand the formula for $v_{z0}/\Omega R$ is

$$\frac{v_{z0j}}{\Omega R}=-\pi\sum_{k=1}^{j}\Delta\gamma'_{1k}\frac{R}{r_{01k}}\cot\phi_{01,k} \tag{2-2}$$

$v_{z01}/\Omega R$ is the induced velocity parallel to the rotating axis of a propeller at radius r_{01}/R, and is induced by the vortex cylinders outside this radius, because v_{z0} of Eq. (2-2) is zero for the cylinders outside the radius according to Eq, (1-4). Therefore the vortex cylinders which has contribution to v_{z0j}/R are the cylinders, the radii of which are larger than r_{0j}/R (see Fig.2-1).

For the tip vortex cylinder, the values of $r_{0\,1,1}/R$ or $r_{0\,1/2}/R$ is equal to one. $r_{0\,1/2}/R$ or $r_{01,1}/R$ can also be witten, as seen in Fig. 2-1, as $(r_{00}/R+r_{01}/R)/2$. Eq. (2-2) in the case of k is 1, therefore, $v_{z01}/\Omega R$ becomes

$$v_{z01}/\Omega R=\Delta\gamma_1'\frac{1}{\frac{r_{01,1}}{R}}\cot\phi_{01,1}{}^{\circ}\cdot(-\pi) \tag{2-3}$$

This equation is written, according to Fig. 2-1 and Fig. 1-2,

$$v_{z01}/R=-\pi(\gamma'_{00}-\gamma'_{01})\frac{1}{\left(\frac{r_{00}}{R}+\frac{r_{01}}{R}\right)\Big/2}\;\frac{\left\{\left(\frac{r_{00}}{R}+\frac{v_{t00}}{\Omega R}\right)+\left(\frac{r_{01}}{R}+\frac{v_{t01}}{\Omega R}\right)\right\}\Big/2}{\left(\frac{v_{z00}}{\Omega R}+\frac{v_{z01}}{\Omega R}\right)\Big/2} \tag{2-4}$$

where the authors assume that tangential and axial velocity components relative to the blade element is the mean values of those values at the two points situated on both sides of this point. Rearranging this equation and using the expression for $v_{t0}/\Omega R$

$$\left(\frac{v_{z01}}{\Omega R}\right)^2=2\pi\gamma'_{01}-2\pi^2\frac{1}{\left(\frac{r_{01}}{R}\right)}\cdot\frac{1}{\frac{r_{01}}{R}+\frac{r_{00}}{R}}\cdot\gamma'_{01}{}^2 \tag{2-5}$$

where the condition of $\gamma'_{00}=0$ is used, because the point located on a cylinder of radius r_{00}/R is outside of propeller blade so that the circulation is zero (see Fig. 2-1). Moreover, if we considered that $(r_{00}/R+r_{01}/R)/2=1.0$, Eq. (2-5) becomes

$$(v_{z01}/\Omega R)^2=2\pi\gamma'_{01}-\pi^2\frac{1}{\left(\frac{r_{01}}{R}\right)}\gamma_{01}'^2 \tag{2-6}$$

Some consideration will be given about the way how to compose $v_{t0}/\Omega R$, which is the tangential component of induced velocity on the tip vortex cylinder, as follows: From Eq. (2-1) and Eq. (1-5-(b))

$$\begin{aligned}
v_{t01/2}/R &= -\pi\left(R/r_{01/2}\right)\gamma'_{01}+\left(-\frac{\pi}{2}\right)(\gamma'_{00}-\gamma'_{01})R/r_{01/2}\\
&= -\pi\frac{1}{\frac{r_{01/2}}{R}}\gamma'_{01}+\frac{\pi}{2}\frac{2}{\frac{r_{00}}{R}+\frac{r_{01}}{R}}\gamma'_{01}\\
&= -\pi\left\{\frac{2}{\frac{r_{00}}{R}+\frac{r_{01}}{R}}-\frac{1}{\frac{r_{00}}{R}+\frac{r_{01}}{R}}\right\}\gamma'_{01}\\
&= \pi\left\{1-\frac{1}{2}\right\}\gamma'_{01}\\
&= -\frac{\pi}{2}\gamma'_{01}
\end{aligned} \tag{2-7}$$

On the other hand, if we consider that the induced velocity of tangential component at r_0/R is the mean of the values at r_{00}/R and r_{01}/R, the expression for $v_{t01/2}/\Omega R$ is

$$\begin{aligned}
v_{t0\,1/2}/\Omega R &= \left(\frac{v_{t00}}{\Omega R}+\frac{v_{t01}}{\Omega R}\right)/2\\
&= \left\{0+(-\pi)\frac{1}{\frac{r_{01}}{R}}\gamma'_{01}\right\}/2=-\frac{\pi}{2}\frac{1}{\left(\frac{r_{01}}{R}\right)}\gamma'_{01}
\end{aligned} \tag{2-8}$$

Comparing Eq. (2-7) with Eq. (2-8), a little difference is found between them. This is the difference between $r_{0\,1/2}/R$ or $(r_{00}/R+r_{01}/R)/2$ and r_{01}/R.

If we adopt the value of Eq. (2-7), the value of $v_{t01/2}/\Omega R$ is underestimated with regard to both r_0/R and γ'_{01}, because $\gamma_0'_{1/2}$ at $r_{0\,1/2}/R(=1.0)$ is larger than γ'_{01} for most of propellers of infinite number of blades. The latter case of Eq. (2-8) shows overestimated values of $v_{t01/2}/\Omega R$ with respect to r_0/R but underestimated for γ_0'. However the errors in $v_{t0}/\Omega R$ may be smaller in both of the cases. Accordingly the authors used the latter relation of Eq. (2-8) in the construction cot $\phi_{01,1}$ in Eq. (2-4).

Next, the expression for $v_{z02}/\Omega R$ will be derived in terms of $\gamma_0{}'_i$. In the same way as the case of Eq. (2-6),

$$\frac{v_{z02}}{\Omega R}=-\pi\frac{\{(r_{00}/R+v_{t00}/\Omega R)+r_{01}/R+v_{t01}/\Omega R)\}/2}{(v_{z00}/\Omega R+v_{z01}/\Omega R)/2}\frac{1}{(r_{00}/R+r_{01}/R)\ /2}(\gamma_0{}'_0-\gamma_0{}'_1)$$

$$-\pi\frac{\{(r_{01}/R+v_{t01}/\Omega R)+(r_{02}/R+v_{t02}/\Omega R)\}/2}{(v_{z01}/\Omega R+v_{z02}/\Omega R)/2}\cdot\frac{1}{\left(1/\frac{r_{01,\,2}}{R}\right)}(\gamma_0{}'_1-\gamma_0{}'_2)$$

$$=\frac{v_{z01}}{\Omega R}-\pi\frac{\{(r_{01}/R+r_{02}/R)+(v_{t01}/R+v_{t02}/R)\}/2}{(v_{z01}/\Omega R+v_{z02}/\Omega R)/2}\cdot\frac{2}{\frac{r_{01}}{R}+\frac{r_{02}}{R}}(\gamma_0{}'_1-\gamma_0{}'_2)$$

Therefore,

$$\left(\frac{v_{z02}}{\Omega R}\right)^2=-2\pi(\gamma_0{}'_1-\gamma_0{}'_2)+\left(\frac{v_{z01}}{\Omega R}\right)^2-2\pi\left\{\frac{v_{t01}}{\Omega R}+\frac{v_{t02}}{\Omega R}\right\}\cdot\frac{1}{\frac{r_{01}}{R}+\frac{r_{02}}{R}}(\gamma_0{}'_1-\gamma_0{}'_2)$$

Replacing $v_{t0}\ /\Omega R$ with the expression of Eq. (2-1) and using Eq. (2-5), we have

$$\left(\frac{v_{z02}}{\Omega R}\right)^2=\left(\frac{v_{z01}}{\Omega R}\right)^2-2\pi(\gamma_{01}'-\gamma_{02}')+2\pi^2\frac{\left(1/\frac{r_{02}}{R}\gamma_{02}'+1/\frac{r_{01}}{R}\cdot\gamma_{01}'\right)}{\frac{r_{01}}{R}+\frac{r_{02}}{R}}(\gamma_0{}'_1-\gamma_0{}'_2)$$

$$=\left(\frac{v_{z01}}{\Omega R}\right)^2-2\pi\gamma_{01}'+\frac{2\pi^2}{\frac{r_{00}}{R}+\frac{r_{01}}{R}}\left(\frac{1}{\frac{r_{01}}{R}}\right)\gamma_{01}'^2-\frac{2\pi^2}{\frac{r_{00}}{R}+\frac{r_{01}}{R}}\cdot\frac{1}{\frac{r_{01}}{R}}\gamma_{01}'^2+\frac{2\pi^2}{\left(\frac{r_{01}}{R}+\frac{r_{02}}{R}\right)}\cdot\frac{1}{\frac{r_{01}}{R}}\gamma_{01}'^2$$

$$+2\pi^2\frac{1/\frac{r_{02}}{R}-1/\frac{r_{01}}{R}}{\frac{r_{01}}{R}+\frac{r_{02}}{R}}\gamma_{01}'\gamma_{02}'-\frac{2\pi^2/\frac{r_{02}}{R}\gamma_{02}'^2}{\frac{r_{01}}{R}+\frac{r_{02}}{R}}+2\pi\gamma_0{}'_2$$

$$=2\pi^2\left\{\frac{1}{\frac{r_{01}}{R}}\cdot\left(\frac{1}{\frac{r_{01}}{R}+\frac{r_{02}}{R}}-\frac{1}{\frac{r_{00}}{R}+\frac{r_{01}}{R}}\right)\gamma_{01}'^2+\left(\frac{1/\frac{r_{02}}{R}-1/\frac{r_{01}}{R}}{\frac{r_{01}}{R}+\frac{r_{02}}{R}}\right)\gamma_{01}'\gamma_{02}'\right.$$

$$\left.-\frac{R}{r_{02}}\cdot\frac{\gamma_{02}'}{\frac{r_{01}}{R}+\frac{r_{02}}{R}}\right\}+2\pi\gamma_{02}'$$

Therefore we obtain

$$\left(\frac{v_{z02}}{\Omega R}\right)^2=2\pi^2\left\{\frac{1}{\frac{r_{01}}{R}}\left(\frac{1}{\frac{r_{01}}{R}+\frac{r_{02}}{R}}-\frac{1}{\frac{r_{00}}{R}+\frac{r_{01}}{R}}\right)\gamma_{01}'^2+\left(\frac{1/\frac{r_{02}}{R}-1/\frac{r_{01}}{R}}{\frac{r_{02}}{R}+\frac{r_{01}}{R}}\right)\gamma_{01}'\gamma_{02}'\right.$$

$$\left.-\frac{1}{\frac{r_{02}}{R}}\frac{\gamma_{02}'^2}{\frac{r_{01}}{R}+\frac{r_{02}}{R}}\right\}+2\pi\gamma_{02}' \tag{2-9}$$

In a similar manner

$$\left(\frac{v_{z03}}{\Omega R}\right)^2=2\gamma_{02}'+2\pi^2\left\{\frac{R}{r_{01}}\left(\frac{1}{\frac{r_{01}}{R}+\frac{r_{02}}{R}}-\frac{1}{\frac{r_{00}}{R}+\frac{r_{01}}{R}}\right)\gamma_{01}'+\frac{R}{r_{02}}\left(\frac{1}{\frac{r_{02}}{R}+\frac{r_{03}}{R}}\right.\right.$$
$$\left.-\frac{1}{\frac{r_{01}}{R}+\frac{r_{02}}{R}}\right\}\gamma_{02}'^2-\frac{R}{r_{03}}\left(\frac{1}{\frac{r_{01}}{R}+\frac{r_{03}}{R}}\right)\gamma_0'{}_3^2+\left(\frac{1/\frac{r_{01}}{R}-1/\frac{r_{01}}{R}}{\frac{r_{01}}{R}+\frac{r_{02}}{R}}\gamma_{01}'\gamma_{02}'\right.$$
$$\left.\left.+\frac{1/\frac{r_{03}}{R}-1/\frac{r_{02}}{R}}{\frac{r_{02}}{R}+\frac{r_{03}}{R}}\gamma_{02}'\gamma_{03}'\right)\right\} \tag{2-10}$$

Thus the general form for $(v_{z0j}/\Omega R)$ is obtained as follows;

$$\left(\frac{v_{z0j}}{\Omega R}\right)^2=2\pi\gamma_{0j}'+2\pi^2\left\{\frac{1}{\frac{r_{01}}{R}}\left(\frac{1}{\frac{r_{02}}{R}+\frac{r_{02}}{R}}-\frac{1}{\frac{r_{00}}{R}+\frac{r_{01}}{R}}\right)\gamma_0'{}_1^2+\frac{1}{\frac{r_{02}}{R}}\left(\frac{1}{\frac{r_{02}}{R}+\frac{r_{03}}{R}}\right.\right.$$
$$\left.-\frac{1}{\frac{r_{01}}{R}+\frac{r_{02}}{R}}\right)\gamma_0'{}_2^2+\cdots\cdots+\frac{1}{\frac{r_{0j-1}}{R}}\left(\frac{1}{\frac{r_{0j-1}}{R}+\frac{r_{0j}}{R}}-\frac{1}{\frac{r_{0j-2}}{R}+\frac{r_{0j-1}}{R}}\right)\gamma_{0j-1}^2$$
$$-\frac{1}{\frac{r_{0j}}{R}}\cdot\frac{1}{\frac{r_{0j-1}}{R}+\frac{r_{0j}}{R}}\cdot\gamma'_{0j}{}^2+\frac{1/\frac{r_{02}}{R}-1/\frac{r_{01}}{R}}{\frac{r_{01}}{R}+\frac{r_{02}}{R}}\cdot\gamma_{01}'\gamma_{02}'$$
$$+\frac{1/\frac{r_{03}}{R}-1/\frac{r_{02}}{R}}{\frac{r_{02}}{R}+\frac{r_{03}}{R}}\gamma_{02}'\gamma_{03}'+\frac{1/\frac{r_{0j-1}}{R}-1/\frac{r_{0j-2}}{R}}{\frac{r_{0j-2}}{R}+\frac{r_{0j-1}}{R}}\gamma_{0j-2}'\gamma_{0j-1}'$$
$$\left.+\frac{1/\frac{r_{0j}}{R}-1/\frac{r_{0j-1}}{R}}{\frac{r_{0j-1}}{R}+\frac{r_{0j}}{R}}\gamma_{0j-1}'\cdot\gamma_{0j}'\right\} \tag{2-11}$$

where $\gamma_0'{}_0=0$, $\gamma_0'{}_{n+1}=0$ and $j=1, 2\cdots\cdots\cdots\cdots$ n.

In Eq. (2-11) the terms of second order in γ_0' show the effect $v_{t0}/\Omega R$. In general, it is well known that for small advance ratio $v_{t0}/\Omega R$ is so small that they will have little contribution to the performance of a propeller. Therefore, for the present static working state, $v_{t0}/\Omega R$ may be neglected.

In this case Eq. (2-11) becomes

$$\begin{aligned}(v_{z01}/\Omega R)^2&=2\pi\gamma_{01}'\\(v_{z02}/\Omega R)^2&=2\pi\gamma_{02}'\\&\vdots\\(v_{z0j}/\Omega R)^2&=2\pi\gamma_0'{}_j\end{aligned} \tag{2.12}$$

$$\vdots$$

$$(v_{z0n}/R)^2=2\pi\gamma_{0n}'$$

From this system of equations, we find that the axial induced velocity $v_{z0}/\Omega R$ at r_0/R is determined solely by γ_0' which is the strength of bound vortex around the blade element at r_0/R. It is an interesting fact that independency of each blade element is assured if v_{t0}/R is neglected.

The considerably good agreement of the present theory with the experiment which will be shown later, might be due to this independency of blade elements. In other words, the calculated distributions of $dC_T/d\left(\frac{r_0}{R}\right)$ and $dC_P/d\left(\frac{r_0}{R}\right)$ over the range of $r_0/R=0.3$ to 0.75 are not affected by the discrepancy of the theoretical flow fields of infinite number of blades near the tips from the actual ones. This fact might be due to this independency of every blade element shown by Eqs. (2-12).

Now putting Eq. (2-1) into Eq. (1-6), and expressing it according to stepwise distribution of Fig. 2-1, we obtain

$$\gamma_{0j}'=\left(\frac{ks}{2}\right)_j\left(\frac{r_{0j}}{R}\right)\sqrt{\left(\frac{v_{z0j}}{\Omega R}\right)^2+\left(\frac{r_{0j}}{R}-\pi\gamma'_{0j}/(r_{0j}/R)\right)^2}\cdot$$

$$\cdot\left\{\frac{\beta_j^0+|\alpha_0^0|}{57.29578^0}-\frac{1}{57.29578^0}\left(\arctan\frac{v_{z0j}}{r_{0j}/R-\pi\gamma'_{0j}(r_{0j}/R)}\right)^0\right\} \quad (2\text{-}13)$$

If $v_{t0}/\Omega R$ is neglected, this equation becomes

$$\gamma'_{0j}=\left(\frac{ks}{2}\right)_j\left(\frac{r_{0j}}{R}\right)\sqrt{\left(\frac{v_{z0j}}{\Omega R}\right)^2+\left(\frac{r_0}{R}\right)^2}\left\{\frac{\beta+|\alpha_0|^0}{57.2958^0}-\frac{1}{57.2958^0}\left(\arctan\frac{v_{z0j}/\Omega R}{r_{0j}/R}\right)^0\right\} \quad (2\text{-}14)$$

The solutions of Eq. (2-11) with Eq. (2-13) or Eq. (2-12) with Eq. (2-14) give the values of $v_{z0}/\Omega R$, γ_0' at r_0/R for the cases of $(v_{t0}/\Omega R)\neq 0$ and $(v_{t0}/\Omega R)=0$ respectively. C_T and C_P are, according to Eq. (1-7)-(a) and (1-7)-(b),

$$C_T=\frac{1}{n}\left|-\pi^4\sum_{j=n}^{1}\gamma_{0j}'\left(\frac{r_{0j}}{R}+\frac{v_{t0j}}{\Omega R}\right)+\frac{\pi^3}{4}\sum_{j=n}^{1}\left\{\left(\frac{v_{z0j}}{\Omega R}\right)^2+\left(\frac{r_{0j}}{R}+\frac{v_{t0j}}{\Omega R}\right)^2\right\}\frac{r_{0j}}{R}\cdot s_j\,c_{dj}\sin\phi_{0j}\right|$$

$$C_P=\frac{1}{n}\left\{\pi^5\sum_{j=n}^{1}\gamma_{0j}'\left(\frac{v_{z0j}}{\Omega R}\right)\left(\frac{r_{0j}}{R}\right)+\frac{\pi^4}{4}\sum_{j=n}^{1}\left\{\left(\frac{v_{z0j}}{\Omega R}\right)^2+\left(\frac{r_{0t}}{R}+\frac{v_{t0j}}{\Omega R}\right)^2\right\}\left(\frac{r_{0j}}{R}\right)^2 s_j\,c_{dj}\cos\phi_{0j}\right.$$

(2-14)

For the case of $(v_{t0j}/\Omega R)=0$,

$$C_T=\frac{1}{n}\left|-\pi^4\sum_{j=n}^{1}\left[\gamma_{0j}'\frac{r_{0j}}{R}-\frac{\pi^3}{4}\left\{\left(\frac{v_{z0j}}{\Omega R}\right)^2+\left(\frac{r_{0j}}{R}\right)^2\right\}\left(\frac{r_{0j}}{R}\right)s_j\,c_{dj}\sin\phi_{0j}\right]\right|$$

$$C_P=\frac{1}{n}\left(\pi^5\sum_{j=u}^{1}\left[\gamma_{0j}'\left(\frac{v_{z0j}}{\Omega R}\right)\cdot\left(\frac{r_{0j}}{R}\right)+\frac{\pi^4}{4}\left\{\left(\frac{v_{z0j}}{\Omega R}\right)^2+\left(\frac{r_{0j}}{R}\right)^2\right\}\left(\frac{r_{0j}}{R}\right)^2 S_j\,c_{dj}\cos\phi_{0j}\right]\right) \quad (2\text{-}15)$$

In Eq. (2–14)$v_{t0j}/\Omega R$ is expressed as $-\pi\frac{1}{\frac{r_{0j}}{R}}\gamma_{0j}'$ according to Eq. (2–1)

§3 METHOD AND RESULTS OF CALCULATION

In the present calculation there is no necessity of successive approximation, and the calculation can be performed either with a slide rule and an abacus or an electronic computer. For example, in the former case Eq. (2–11) and Eq. (2–13) are solved for $j=1$ by graphical method with γ_{01}' as abscissa and $v_{z01}/\Omega R$ as ordinate. The intersection of the two curves represented by Eq. (2–11) and Eq, (2–13) corresponds to the values of γ_{01}' and $v_{z01}/\Omega R$ which satisfies these equations. Then for the case of $j=2$, replacing the γ_{01}' of Eq. (2–9) with the value just obtained above, the similar graphical solution results in $v_{z02}/\Omega R$ and γ_{02}'. $v_{z03}/\Omega R$, γ_{03}' and so on are obtained by the same procedure. If we use Eq. (2–1) together with the above equations, $v_{t0j}/\Omega R$, ϕ_{0j}, c_{lj} etc. can be obtained during the process of the present calculation. $dC_T/d(r_0/R)$ and $dC_P/d(r_0/R)$ are the integrands of Eqs. (2–14) and (2–15) respectively. Integrating these with respect to r_0/R we obtain thrust coefficient C_T and power coefficient C_P. If $v_{t0}/\Omega R$ is neglected, the solution can be performed more easily by using Eq. (2–12) and Eq (2–14).

In the present paper calculation was performed with the electronic computer, OKITAC 5090–H. The number of diviison n of Fig. 2–1 in this case is twenty-

Table 3-1 The propeller used in the present research

r_0/R	β^0	c/R
0.1	82.96	0.340
0.2	58.30	0.315
0.3	22.38	0.290
0.4	17.17	0.265
0.5	13.87	0.240
0.6	11.62	0.215
0.65	10.75	0.203
0.7	10.00	0.190
0.75	9.35	0.178
0.8	8.77	0.165
0.85	8.26	0.153
0.90	7.81	0.140
0.925	7.61	0.134
0.95	7.41	0.128
0.975	7.22	0.121
1.000	7.04	1.150

Number of blades $B=4$

Pitch-diameter ratio$=h/D=\pi\cdot\frac{r_0}{R}\cdot\tan\beta=\pi\times0.7\cdot\tan 10°$

$c/R=\frac{\text{chord length}}{\text{outer radius}}=0.365-0.26\frac{r_0}{R}$

Airfoil: Göttingen 623

Blade angle β is measured from the bottom flat surface of the airfoil

Table 3-2 Göttingen 623 airfoil

α^0	c_l	c_d
-7.17	-0.195	0.255
-5.81	-0.045	0.0147
-4.39	0.092	0.0119
-2.98	0.231	0.0106
-1.55	0.366	0.0106
-0.14	0.505	0.0122
1.25	0.648	0.0139
2.68	0.782	0.0155
4.10	0.919	0.0181
5.57	1.045	0.0224
7.12	1.151	0.0281
8.74	1.240	0.0374
10.60°	1.273	0.0573

α: geometrical angle of attack measured from the bottom straight line
Aspect ratio$=\infty$
$R_e=cv/\nu=4.1\times10^5$
$dc_l/d\alpha=2\pi k=5.56$, $k=0.885$
Zero-lift angle $\alpha_0{}^0=-5.35°$
(from Ergeb. Versuch. Göttingen, IV Lief., S. 57)

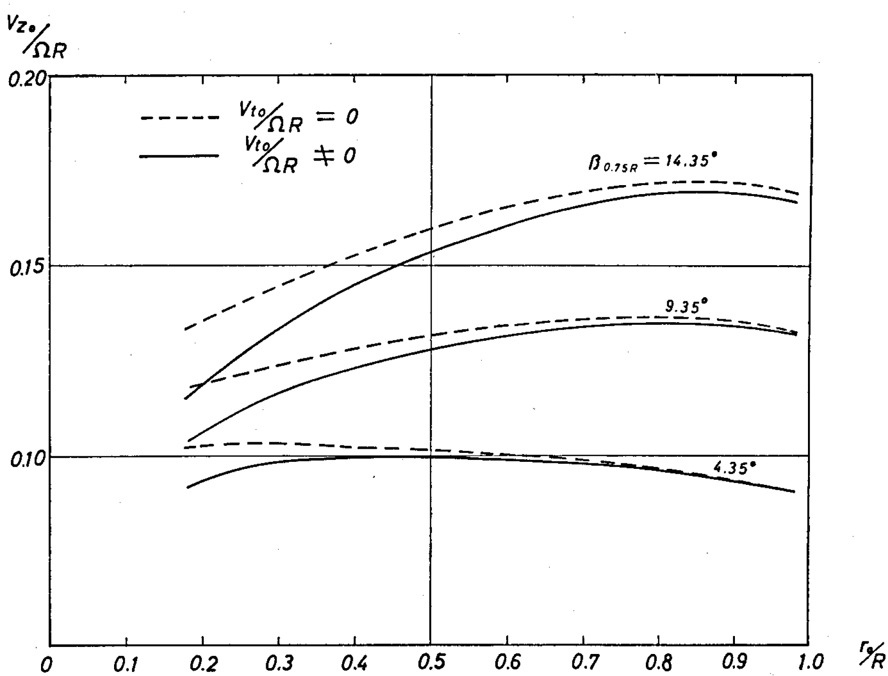

Fig. 3-1 Axial induced velocity (calculated)

four. The propeller used in the present calculation has the principal items shown in Table 3-1, Its blade section used from the root to the tip is Gottingen 623 shown in Table 3-2. The calculated values of $v_{z0}/\Omega R$, $v_{t0}/\Omega R$, γ_0' and c_l are

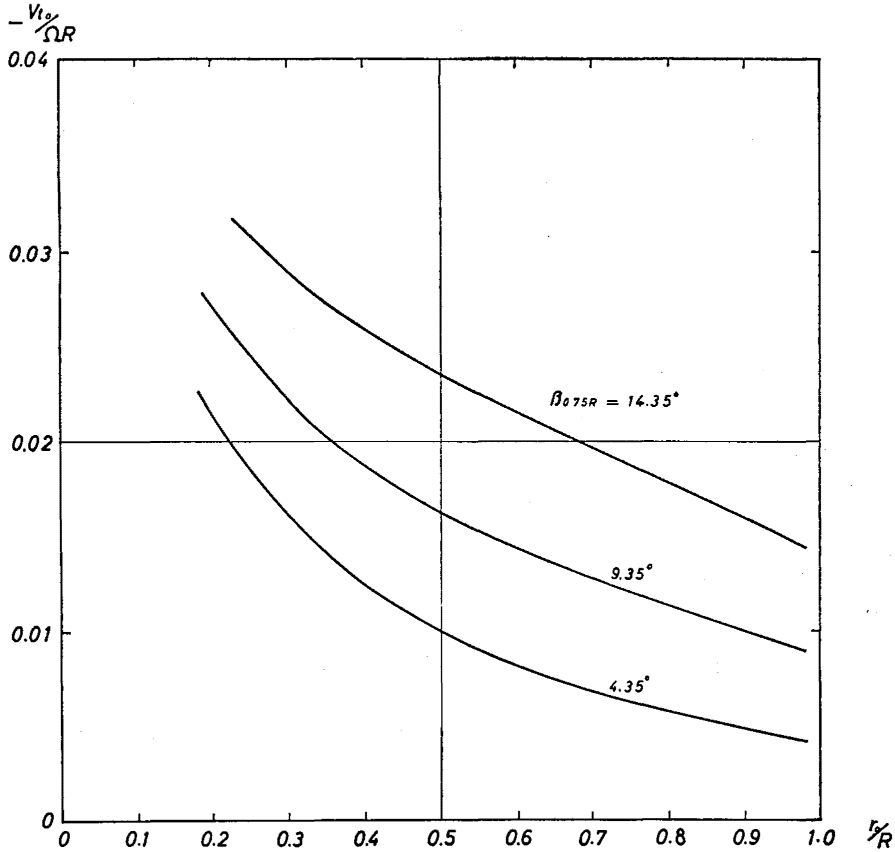

Fig. 3-2 Tangentlal induced velocity (calculated)

in Figs. (3-1) to (3-4) with r_0/R as abscissa. $dC_T/d(r_0/R)$ and $dC_P/d(r_0/R)$ are shown in Figs. 3-5 and 3-6 respectively for those cases in which the term of $v_{t0}/\Omega R$ is taken into consideration and not taken into consideration with and without the term of drag coefficient c_d.

Some discussions of the theoretical results which are considered to be convenient for us to discuss with experimental results will be described in Secrion 4. In the following the results having exclusively theoretical interest will be shown here.

As we expected before the present theoretical calculation, the tangential component of induced velocity $v_{t0}/\Omega R$ is very small in its absolute value but relatively large for small value of r_0/R (see also Fig. 4-3-(a)). As dotted lines of Figs. 3-1 to 3-6 show, the effect of $v_{t0}/\Omega R$ becomes large for the blade elements at small values of r_0/R. The circulation γ_0' around these blade becomes small and consequently, as seen in Figs. 3-5 and 3-6, the values of $dC_T/d(r_0R)$ and $dC_P/d(r_0R)$ are also small. Axial induced velocity of $v_{z0}/\Omega R$ are of the order of

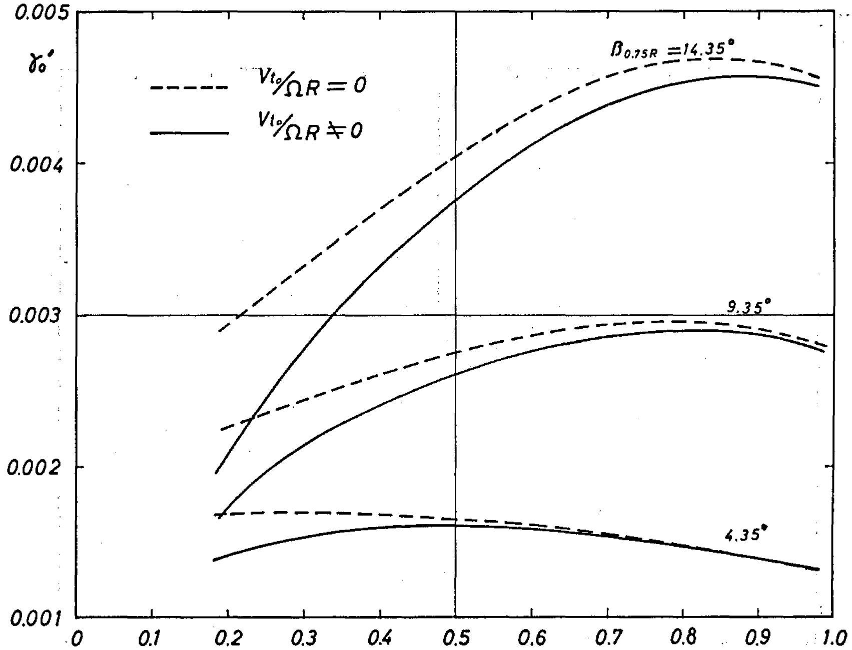

Fig. 3-3 Circulation around blade elements (calculated)

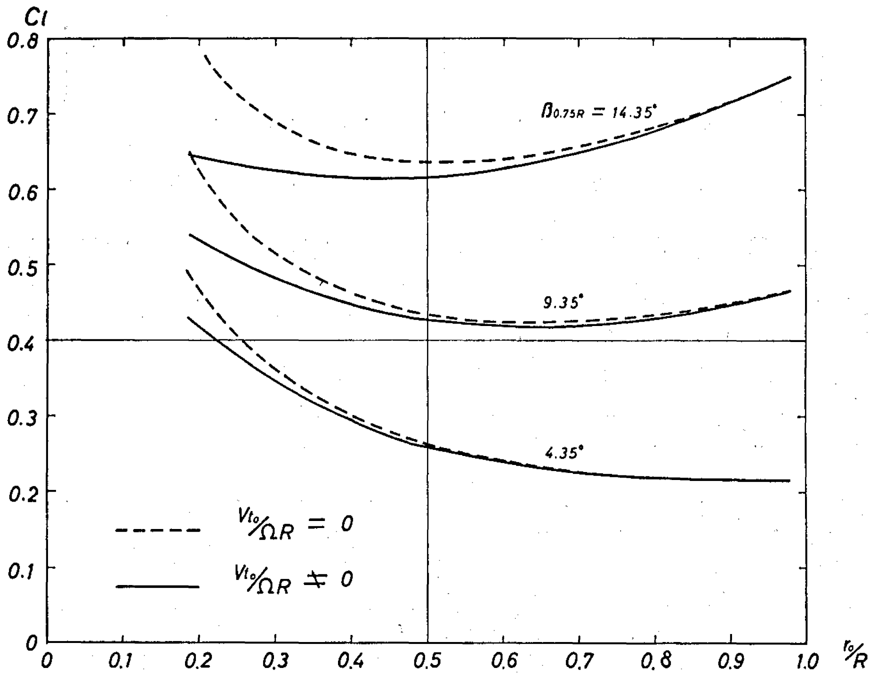

Fig. 3-4 Section lift coefficient (calculated)

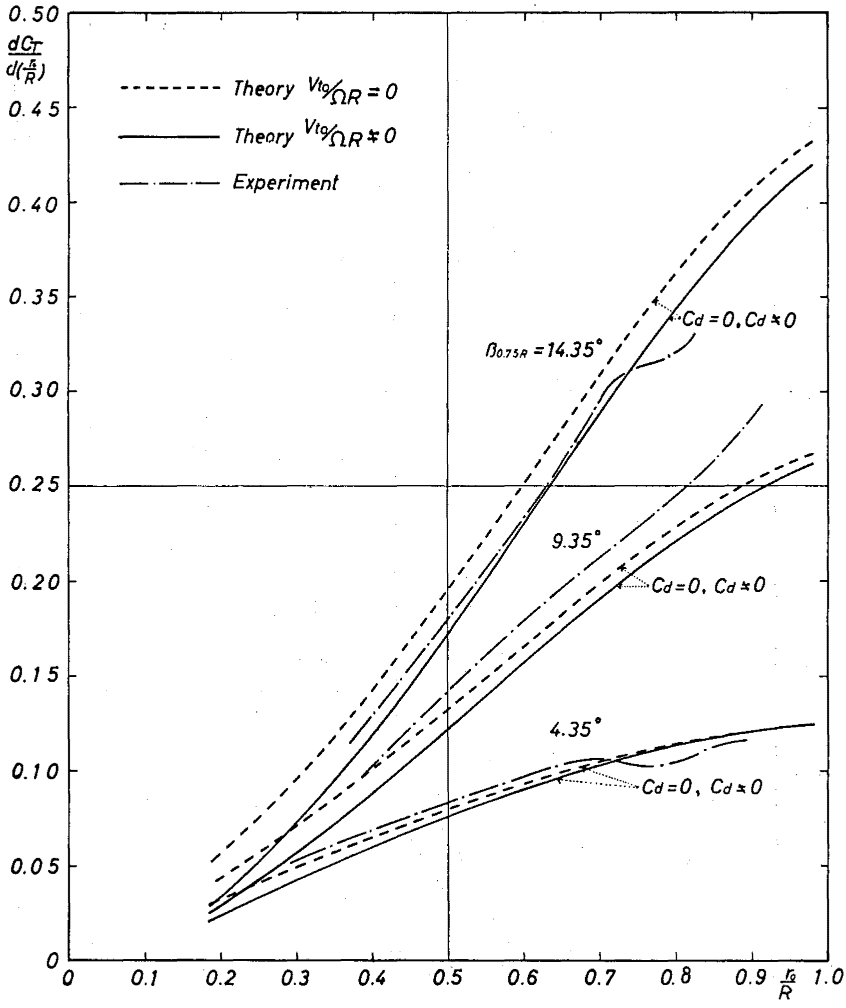

Fig. 3-5 Thrust coefficient grading (calculated and experimental)

0.1 for $\beta_{0.75R}$=4.35°, 0.13 for 9.35° and 0.17 for 14.35° (see Fig. 3-1). We see that $v_{z0}/\Omega R$ is also affected by $v_{t0}/\Omega R$ at small value of r_0/R.

The contribution of profile drag of blade elements to the values of $dC_T/d(r_0/R)$ and $dC_P/d(r_0/R)$ is seen in Figs. 3-5 and 3-6. In calculation the value of c_d or the drag coefficient of blade elements is taken to be the constant value of 0.012 for the simplification of calculation. From the inspection of these figures it can be seen that the effect of c_d on thrust coefficient grading is very small, while the effect on the power coefficient grading is considerably large. In the tables of (a), (b) and (c) of Table 4-1, which will be shown later, the values of C_T, C_P and Figure of Merit F. M. $=0.798 \cdot C_T/C_P$ are shown. The former two kinds of values were obtained by the integration of the values of $dC_T/d(r_0/R)$

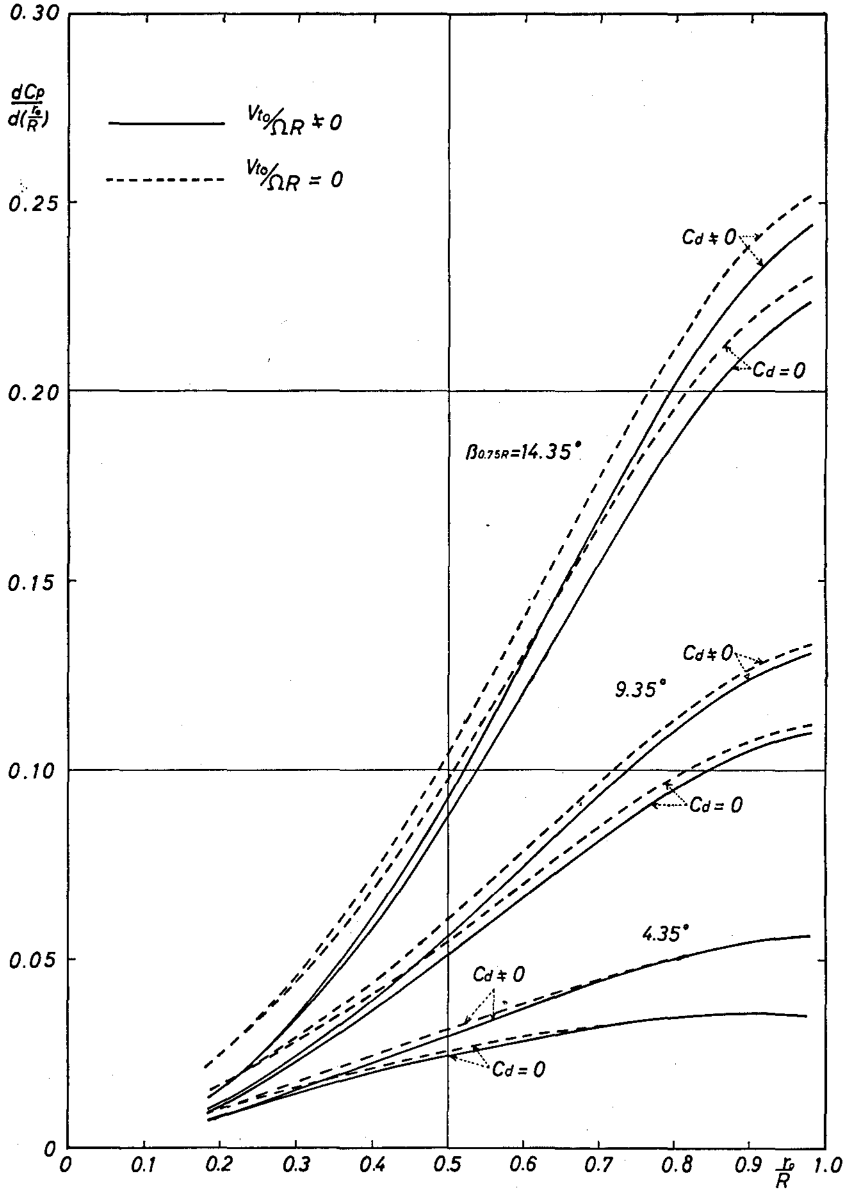

Fig. 3-6 Power coefficient grading (calculated)

and $dC_P/d(r_0/R)$ shown in Figs. 3-5 and 3-6 with respect to r_0/R from 0.185 to 1.0. In the table of (a) the column of ΔC_{Td} shows that C_T decreases by about one per cent by the effect of c_d. On the other hand the column of ΔC_P of the table of (b) means that c_d increases C_P by the order of thirty six per cent

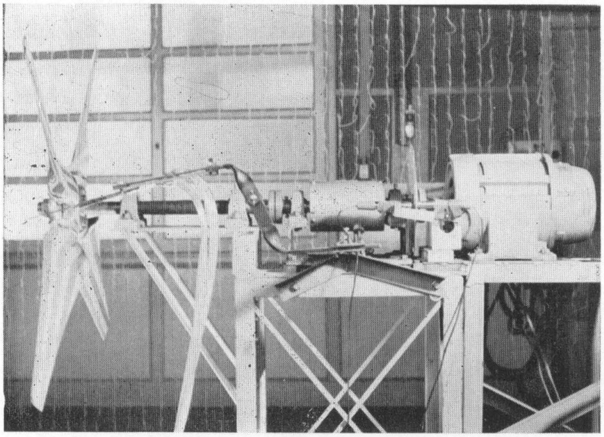

(a)

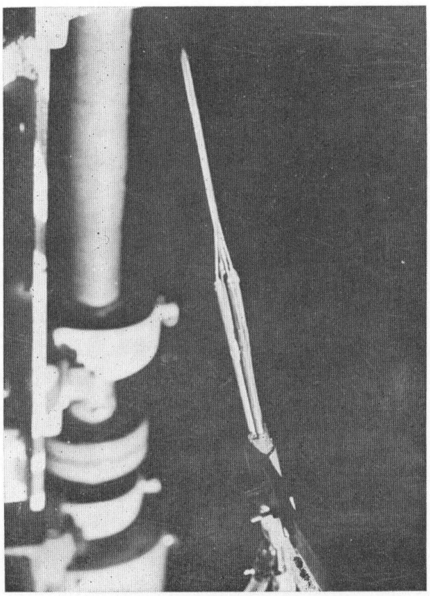

(b)

Fig. 4-1 (a) Experimental apparatuses and propeller
(b) Five-holes Pitot tube $2\times2\times100$ (in m/m)

for $\beta_{0.75R}=4.35°$ and ten per cent for 14.35°. As seen from the table of (c), F. M. decreasses by twenty to nine per cent due to the effect of c_d. Therefore it can be concluded that the section drag coefficient c_d has much effect on C_P and F. M..

Now we shall see the distribution of lift coefficient c_l along blades. c_l or section lift coefficient is about 0.2 for the propeller of $\beta_{0.75R}=43{\cdot}5°$, about 0.4 for 9.35° and 0.7 for 14.35° (see Fig. 3-4). In the last case the working condition of the airfoil sections or blade elements, especially near the root and near the tip, approaches its stalling condition.

The theoretical results of which discussions have not performed here, as previously stated, will be considered in the next section of experimetal results.

§4 Experimental Apparatuses, Method of Evaluation of the Experimental Results and Discussion about Them

The general arrangement of the experiment is shown in Fig. 4-1-(a) and (b). The experiments were performed with a wooden, four-bladed model propeller of the diameter of one meter. The pitch angle distribution and blade width distribution are given in Table 3-1. By loosening the bolts clamping the roots of blades, pitch angle can be changed. This propeller has the same nondimensional form as the one used in the previous numerical calculation. As shown in Fig. 4-1, an A.C. 100 volt repulsion motor of about 0.75 KW at 1,700 rpm with four poles drives the propeller. The number of rotation of this motor can be changed with a slidac. The number of rotation mainly selected in the present experiment is about 1,000 rpm. The Reynolds number based on the chord of seventy-five per cent radius is of the order of 3.0×10^5. The airofoil data shown in Table 3-2 is of the same order of magnitude of Reynlods number, so that the authors used this data as the section characteristics of the present propeller. Torque was measured with a strain gauge torque meter by Kyowa Electric Co. Ltd., which was set between the propeller and the motor as shown in Fig. 4-1-(a). Thrust coefficient grading $dC_T/d(r_0/R)$ was obtained by traversing the slipstram with a five-hole total head tube which was aligned with the direction of local flow. The form and arrangement of traversing are shown in Figs. 4-1-(a) and (b). The whole system of the propeller and motor can be suspended from a frame, when thrust is measured by a load cell. Number of rotation was measured with a photocell tachometer connected to an electronic counter. The Pitot traverse with the total head tube was performed at the position behind the trailing edge of blades by 0.015 meter (Fig. 4-2). Measurements were performed for three kinds of blade-pitch-angles $\beta_{0.75R}=4.35°$, 9.35° and 14.35°. Visualizing the flow field by woolen threads and smoke of kerosene, photographs of flow field behind the propeller was taken and is shown in Fig. 4-3. Thus the regions of normal, reverse and vortex flows were inspected by these flow visualization, while the direction of flow was read with the five-hole Pitot tube (the meaning of suffex θ here defined is different from the one shown in Fig. A-1).

The thrust coefficient grading obtained from the experiment stated above is shown by lines consisting of alternate long and short dashes in Fig. 3-6, together

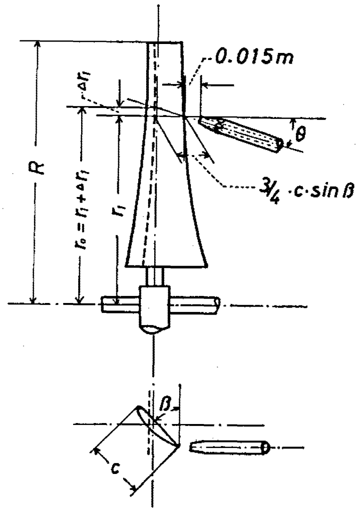

Fig. 4-2 Determination of radino corresponding to total head incvease

with the theoretical curves. In evaluating $dC_T/d(r_0/R)$ from experimental data the relation of

$$\frac{dC_T}{d\left(\frac{r_0}{R}\right)} = \cos^2\phi_0 \cdot \frac{\pi}{8} \cdot \frac{\left(\frac{r_0}{R}\right)}{\rho\pi^2 R^2} \Delta h \tag{4-1}$$

was used. In this equation Δh is the difference of total head h_r behind the propeller from the total head in front of the propeller h_f which is equal to atmospheric pressure in our case of static condition. $\cos^2\phi_0$ is a correction factor derived for the case of static condition by the authors according to Pankhurst's paper[11).* ϕ_0 is the direction of inflow relative to a blade element at radius of r_0 and here theoretical value calculated by the present theory was used. The value of $dC_T/d\left(\frac{r_0}{R}\right)$ does not mean the one at r_1/R where the five-hole total head tube is located. Considering the contraction of flow in slipstream, the increase in total head at that r_1/R must be produced from $r_1/R + \Delta r_1/R$ (see Fig. 4-2). In the vortex theory of a wing the wing is replaced by a vortex line located at quarter chord from leading edge. According to this manner the intersection of the line inclining to the axis of rotation by the angle of $\theta°$ and drawn from the point of measurement of total head with the line connecting the quarter chord points of every blade element was considered to be the point where Δh was produced. The value of $dC_T/d\left(\frac{r_0}{R}\right)$, therefore, was refered to $r_1/R + \Delta r_1/R$ and plotted in Fig. 3-6 by reading r_0/R for $r_1/R + \Delta r_1/R$. In this correction, as seen in the lower figure of Fig. 4-2, the Pitot tube is arranged in parrallel with the direction of

* See Appendix A.

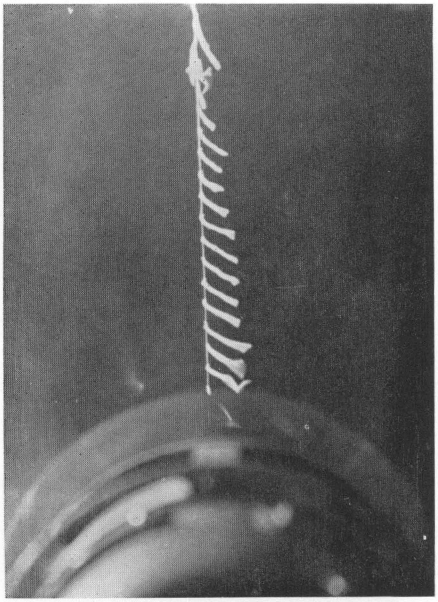

(a)

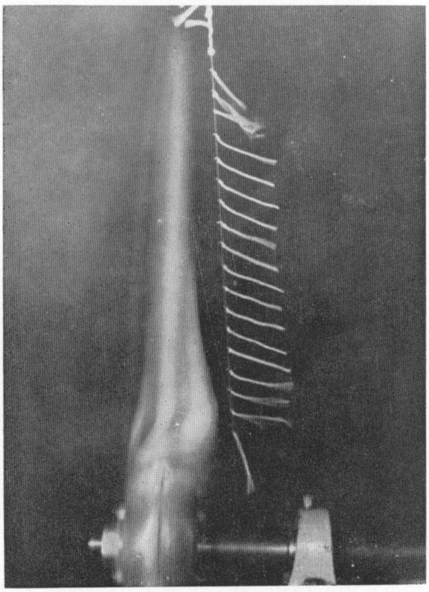

(b)

Fig. 4-3 (a) Flow seen from lee, tangential component of induced velocity increases to root, near tip flow is unstable, full of vortices or reversed

(b) Side view of flow just behind propeller, $\frac{r_0}{R} \doteqdot 0.75 \sim \frac{r_0}{R} = 1.0$ flow is unstable, full of vortices

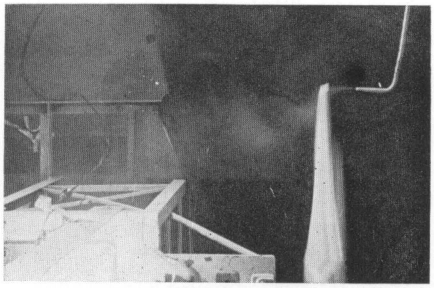

(c)

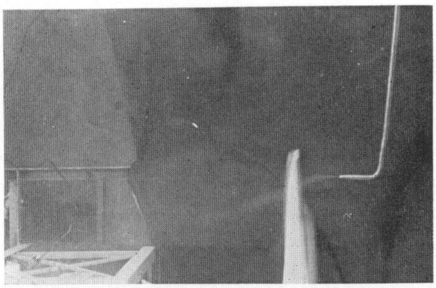

(d)

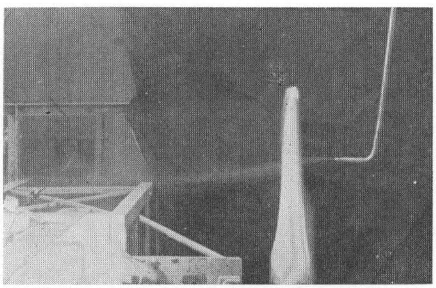

(e)

Fig. 4-3 (c) unstabel flow region near tip
(d) boundary of normal and unstable flows
(e) stable normal stream line

the axis of the propeller, because the tangential component of induced velocity is so small that the errors of the total head due to the tangential inclination of flow may be negligibly small.

The present theory, as stated before, is based on the unrealistic assumption of infinite number of blades. If we take this fact into consideration, the experimental curves of Fig. 3-5 agree with the theoretical ones in considerable degree in the range from $r_0/R=0.3$ to $r_0/R=0.75$. Beyond this region, up to $r_0/R=1.0$ the experimental values lose their reliability, because in this region the flow is reverse or full of vortices (see Fig. 4-3-(a), (b) and (c)). On the other hand in this region the present theory, which is composed on the assumption of infinite number of blades, cannot say anything, because it does not include tip effect of a propeller which is very much predominant factor for the real propeller performances near the tip of it. Hence the comparison of the experimental results of the total head tube with the present theory should be restricted to comparatively inner side of radius where the effect of the the tips of a propeller, vortex flow, reverse flow etc, near the tips have negligible effect. The experimental curves of $dC_T/d(r_0/R)$ in Fig. 3-5 are located rather near the theoretical ones of $(v_{to}/\Omega R)=0$ for $\beta_{0.75R}=4.35°$, while they are nearer to the curve of $(v_{to}/\Omega R)\neq 0$ for 14.35°. The authors cannot explain why the case of 9.35° shows the largest discrepancy among these angles. It is usual that experimental value is less than theoretical value. In the present case the experimental curves are all located above the theoretical ones. The authors, however, do not consider this irregularity to be irrational. The reasons are as follows: 1) the methods of researches of propellers of static condition are not yet settled, so that, as seen in Gartshore's[4] paper, the distribution curves of $dC_T/d(r_0/R)$ and $dC_P/d(r_0/R)$ may fluctuate by the present order of magnitude due to the assumption and method used

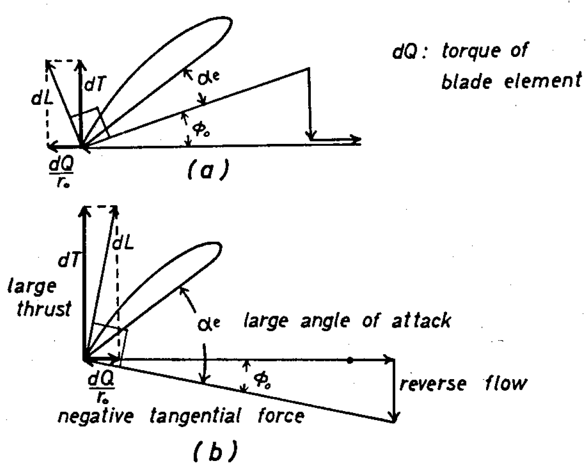

Fig. 4-4 (a) normally working state
(b) windmilling state of blade element of propeller at static condition

Table 4-1. Comparison of theoritical values of C_T, T_P and F.M. with experimental ones

(a)

$\beta^{\circ}_{0.75R}$	C_T					$\Delta C_T = \frac{C_{T\mathrm{exp}} - C_{T\mathrm{the}}}{C_{T\mathrm{the}}} \times 100\%$		$\Delta C_{Td} = \frac{C_{T\mathrm{the}②} - C_{T\mathrm{the}③}}{C_{T\mathrm{the}③}} \times 100\%$
	Experimental values measured with load cell	Theoretical values (integrated from $r_0/R=0.185$ to 1.0)						
		$v_{to}/\Omega R \neq 0$		$v_{to}/\Omega R = 0$				
		$c_d=0.012$	$c_d=0$	$c_d=0.012$	$c_d=0$			
	①	②	③	④	⑤	①−②	①−④	②−③
4.35	0.0645	0.0682	0.0688	0.0716	0.0723	−5	−10	−1
9.35	0.100	0.1237	0.1244	0.132	0.133	−17	−24	−1
14.35	0.174	0.186	0.187	0.203	0.204	−7	−14	−1

(b)

$\beta^{\circ}_{0.75R}$	C_p					$\Delta c_p = \frac{C_{p\mathrm{exp}} - C_{p\mathrm{the}}}{C_{p\mathrm{the}}} \times 100\%$		$\Delta c_{pd} = \frac{C_{P\mathrm{the}②} - C_{P\mathrm{the}③}}{C_{P\mathrm{th}③}} \times 100\%$
	Experimental values measured with torque meter	Theoretical values (integrated from $r_0/R=0.185$ to 1.0)						
		$v_{to}/\Omega R \neq 0$		$v_{to}/\Omega R = 0$				
		$c_d=0.012$	$c_d=0$	$c_d=0.012$	$c_d=0$			
	①	②	③	④	⑤	①−②	①−④	②−③
4.35	0.0279	0.0288	0.0212	0.0300	0.0222	−3	−7	36
9.35	0.0493	0.0598	0.0523	0.0633	0.0555	−18	−22	14
14.35	0.0991	0.106	0.0980	0.114	0.106	−7	−13	10

(c)

$\beta^{\circ}_{0.75R}$	F. M.					$\Delta F.M. = \frac{F.M._{\mathrm{exp}} - F.M._{\mathrm{the}}}{F.M._{\mathrm{the}}} \times 100\%$		$\Delta F.M._d = \frac{F.M._{\mathrm{the}②} - F.M._{\mathrm{the}③}}{F.M._{\mathrm{the}③}} \times 100\%$
	Experimental values	Theoretical values calculated corresponding to (a) and (b)						
		$v_{to}/\Omega R \neq 0$		$v_{to}/\Omega R = 0$				
		$c_d=0.012$	$c_d=0$	$c_d=0012$	$c_d=0$			
	①	②	③	④	⑤	①−②	①−④	②−③
4.35	0.466	0.496	0.677	0.511	0.693	−6	−9	−20
9.35	0.512	0.576	0.670	0.604	0.695	−11.2	−15	−22
14.35	0.583	0.603	0.660	0.630	0.694	−3	−8	−9

(d)

$\beta^{\circ}_{0.75R}$	$C_{T0.3R\sim0.75R}$					$\Delta C_{T0.3\sim0.75R} = \left(\frac{C_{T\mathrm{exp}} - C_{T\mathrm{the}}}{C_{T\mathrm{the}}}\right)_{0.3\sim0.75R} \times 100\%$	
	Experimental values measured with Pitot tube	Theoretical value (integrated from $r_0/R=0.3$ to 0.75					
		$v_{to}/\Omega R \neq 0$		$v_{to}/\Omega R = 0$			
		$c_d=0.012$	$c_d=0$	$c_d=0.012$	$c_d=0$		
	①′	②′	③′	④′	⑤,	①′−②′	①′−④′
4.35	0.038	0.0349	0.0352	0.0367	0.0370	9	4
9.35	0.067	0.0588	0.0592	0.0636	0.0640	14	6
14.35	0.088	0.0854	0.0859	0.0953	0.0959	3	−8

$F.M.$=Figure of merit=0.798 $(C_T)^{3/2}/C_p$

in that theory, and 2) due to the failure during manufacturing the propeller blades used in the present experiment the blade angle distribution along blades has the error of the order of magnitude of $\pm 0.3°$, so that these errors may be a cause of the discrepancy stated above.

Adams[5] describes that the blade element near the tip of a propeller, as explained in Fig. 4-4, may work as the blade element of a windmill. If the blade element work as this, it would show large thrust grading. Now returning to the experimental curves of Fig. 3-5, we see that three experimental curves show rather large increase at $r_0/R=0.85\sim0.9$ at $r_0/R=0.85\sim0.9$ after some decrease in their amount at $r_0/R=0.75$. This increase may be caused by the windmill state of blade element near the tip of the peopeller. The form of curves, which once decrease and again increase, have something similar to Gartshore's curves of $dC_T/d(r_0/R)$. If the present theory of very simple process without any necessity of successive approximation shows good agreement with every other kind of experiments than the present one, it will give a reliable distribution of $dC_T/d(r_0/R)$ from the root to $r°/R=0.75$. Then application of the elaborate theory of finite number of blades only to the region from $r_0/R=0.75$ to 1.0 will do for the calculation of a propeller.

Next we shall examine the values of C_T, C_P. Table 4-1 shows the experimental and theoretical values of C_T, C_P and *F.M.*, where C_T and C_P of experiment were directly measured with a load cell and a torque meter.* As seen in the column ①−② the experimental values agree with the theoretical ones within the errors of ten per cent except the case of $\beta_{0.75R}=9.35°$. All of these experimental values are less than the theoretical values, so that the valus of $\varDelta C_T$, $\varDelta C_P$ and $\varDelta F.M.$, which are the deviation from theorecical value, are negative except one case. In the column of ①−② of Table 4-1-(d), however, the experimental values are higher than the theoretical ones. These values result from the integration of $dC_T/d(r_0/R)$ of Figs. 3-5 from 0.3 of r_0/R to 0.75 in which region the experimental and theoretical curves of $dC_T/d(r_0/R)$ agree with each other in considerable degree. The measured values integrated all over the propeller disc, however, as stated above, are lower than the theoretical values. This change from positive to negative may be mainly due to the state of flow field near the blade tip, where the present theory cannot be correct and the experimental results of Pitot traverse are not reliable.

Anyhow, it may be said that the theoretical curves agree with the experimental ones with the error of ± 10 per cent except the case of $\beta_{0.75R}=9.35°$. The authors think that the errors of the order stated above may be allowable considering the assumption used in the present theory and the informations so far obtained about the flow around the propeller of static condition.

As seen in Adams'[5] paper and from the present theoretical and experimen-

---

* As stated before, the results with total head tube are not shown in the tables of (a), (b) and (c), because the total head showed very much unstable or negative values near the tip, so that C_T calculated including the erroneous values obtained in this region are not reliable.

tal results, there remain many problems, for example, reverse flow, windmill state etc., to be solved in the region near the tip of a propeller at its static condition. The authors would like to say that the region where the investigations of a propeller of static state should be concentrated is the region ranging from $r_0/R=0.75$ to $r_0/R=1.0$.

Conclusions

Theoretical investigations of a propeller at its static working state was performed by a vortex theory based on the assumption of infinite number of blades.

Experiments were performed with a four-bladed propeller at the blade-angles, measured at $0.75R$, of 4.35°, 9.35° and 14.35°.

The following are the results obtained from theoretical investigation;

1) Thrust coefficient and torque coefficient gradings can be calculated without the method of successive approximation.

2) Tangential component of induced velocity, though small in its absolute magnitude compared with axial component, has considerable effect on circulation around blade elements, thrust coefficient grading and power coefficient grading and its effect is stronger on the blade element of smaller value of radius. Tangential component works on γ_0', $dC_T/d(r_0/R)$ and $dC_P/d(r_0/R)$ so as to reduce these values.

3) The effect of drag coefficient c_d on the performance of a propeller at static state is of appreciable amount for power coefficient C_P and consequently for Figure of Merit *F. M.*, while very small for thrust coefficient C_T.

4) Lift coefficient increases as the blade angle, but up to $\beta_{0.75R}=14.35°$ no blade elements works at its stall condition.

By comparison of theoretical results with experimental ones the following are shown:

5) Theoretical and experimental distributions of $dC_T/d(r_0/R)$ and $dC_P/d(r_0/R)$ with respect to r_0/R agree with considerable accuracy in the range from $r_0/R=0.3$ to 0.75 except the case of $\beta_{0.75R}=9.35°$.

6) The theoreticol values of C_T, C_P and *F. M.* agree within the error of the order of ± 10 per cent with the experimental ones except the case of $\beta_{0.75R}=9.35°$.

7) In the present report nothing can be said about the phenomena in the range of $r_0/R=0.75$ to 1.0, but considerably good agreement in this region ranging $r_0/R=0.3$ to 0.75 suggests the possibility that the performance of a propeller at its static condition may be calculated by the present method of calculation within the error of the order of ten per cent in the region of $r_0/R=0.3$ to 0.75.

The authors think that the region to which the investigations of a propeller performances at its static condition should be concentrated may be the region ranging from $r_0/R=0.75$ to $r_0/R=1.0$.

The authors should like to express their profound gratidude to Mr. H. V. Borst and Dr. D. E. Ordway for their very kind considerations, encouragement and discussions given to the present investigations. The authors' thankfulness are also due to assistants Noda and Okura for their assistance in performing the experiment, to Mr. A. Sakurai, student of doctor course, and Mr. T. Nagayama, student of master course, for their assistances in calculation with an electronic computer and in drawing the figures, and to Mr. Y. Watanabe, student of master course, for his help in performing the experiment.

References

1) D. E. Ordway, J. C. Erickson, Jr., A New Approach to the Static Thrust Problem, Therm Advanced Research, Ithaca, New York, TAR-TR 631 Phase I March 1963, TAR-TR 632 Phase II May 1963, TAR-TR 635 PhaseIII August 1963, and TAR-TR 638 Phase IV December 1963.

2) J. C. Erickson, Jr., R. M. Ladden, H. V. Borst and D. E. Ordway, A. Theory for VTOL Propeller Operation in a Static Condition, USAAVLABS Thechnical Report, 65-69, October 1965, U. S. Army Aviation Material Laboratories.

3) J. C. Erickson, Jr., & D. E. Ordway, A Theory for Static Propeller Performance, Therm Advanced Research, a paper presented at GAL/AVLABS Symposium, "Aerodynamic Problem Associated with V/STOL Aircraft", Baffalo, New York, June 22 to 24, 1966.

4) I. S. Gartshore, An Application of Vortex Theory to Propellers Operating at Zero Advance Ratio, Mechanical Engineering Research Laboratories, McGill University, Montreal, June 1966.

5) G. N. Adams, Propeller Research at Canadair Limited, CAL/USAAVLABS Symposium Proceedings, Aerodynamic Problems Associated with V/STOL Aircraft, Vol. I, Propeller and Rotor Aerodynamics, 22-24 June 1966 (see p. 9).

6) M. Iwasaki, Diagrams for Use in Calculation of Induced velocity by Propellers, Reports of Research Instittute for Applied Mechanics, Kyushu University, Vol. VI, No. 23, 1958, pp. 87-126.

7) M. Iwasaki, Vortex Theory of an Airscrew in Consideration of Contraction or Expansion of Slipstream and Variation of Pich of Vortex Sheets in It, Reports of Research Institute for Applied Mechanics, Kyushu University, Vol. VII, No. 27, 1959, pp. 159-232.

8) C. N. H. Lock, R. C. Pankhurst and J. F. C. Conn, Strip Theory Method of Calculation for Airscrews on High-Speed Aeroplenes A. R. C. TR, Report and Memoranda, No. 2035, Oct, 1945.

9) M. Iwasaki, The Experimental and Theoretical Investigations of Windmills, Reports of Research Intstitute for Applied Mechanics, Kyushu University, Vol. II, No. 8, 1953, pp. 181-229.

10) S. Kawada, Calculation of Induced Velocity by Helical Vortices and its Application to Propeller Theory, Report of the Aeronautical Research Institute, Tokyo Imperial University, No. 172, January 1939.

11) R. C. Pankhurst, Airscrew Thrust Grading by Pitot Traverse: Allowance for Rotation of Slipstream at High Rates of Advance, A. R. C. TR., Report and Memoranda No. 2049, 10th May, 1945.

Appendix-A

In this section Pankhurst's[11] paper is explained for the case of static condition of a propeller.

Axial momentum theory of a propeller, in which tangential component v_{to} is neglected, shows that the integration of the difference of total head Δh, which is the difference of total head behind the propeller h_r from the total head in front of the propeller h_f, results in the thrusts of a propeller. This can be written in formula as follows:

$$\left(\frac{dT}{dr_0}\right)_{v_{to}=0}=2\pi r_0(h_r-h_f)=2\pi r_0 \Delta h \tag{A-1}$$

Eq. (A-1) can be reduced to the non-dimensional form of

$$\left\{\frac{dC_T}{d(r_0/R)}\right\}_{v_{to}=0}=\frac{\pi}{8}\frac{r_0}{R}\frac{\Delta h}{\rho n^2 R^2} \tag{A-2}$$

On the other hand, as seen in Fig. A-1, if we take v_{to} into consideration, airfoil section theory shows that

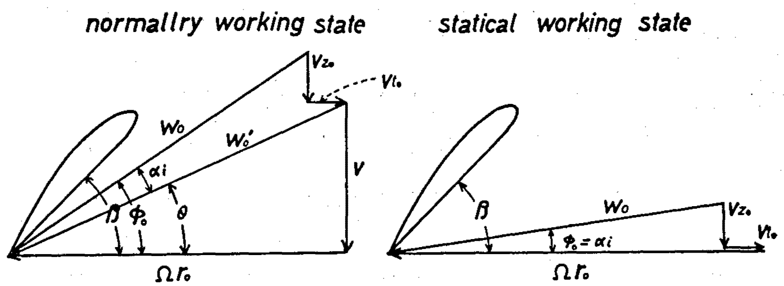

Fig. A-1 Flow diagram of blade element at r_0

$$dL=\rho\Gamma w_0 dr_0 \tag{A-2}$$

Neglecting drag component of the blade element, therefore,

$$dT=B\rho\Gamma w_0 dr_0 \tag{A-3}$$

while the measured total difference across the propeller disc is

$$\Delta h=B\rho\Gamma\Omega/2\pi \tag{A-4}$$

Accordingly, by the substitution of *Eq.* (A-4) into *Eq.* (A-3) we obtain

$$\begin{aligned}\left(\frac{dT}{dr_0}\right)_{\text{true}}&=\frac{w_0}{\Omega r_0}\cos\phi_0\left(\frac{dT}{dr_0}\right)_{v_{to}=0}\\&=\frac{w_0}{w^{0\prime}}\frac{w_0'}{\Omega r_0}\cos\phi_0\left(\frac{dT}{dr_0}\right)_{v_{to}=0}\\&=\frac{\cos\alpha_i\cos\phi_0}{\cos\theta}\left(\frac{dT}{dr_0}\right)_{v_{to}=0}\end{aligned} \tag{A-5}$$

where the suffix "true" means the value in which the effect of v_{to} is included.

In the static working state $\theta=0$ and $\alpha_i=\phi_0$. Nondimensionalizing by the factor $\rho n^2 D^4$ and R, *Eq.* (A-5) is reduced to

$$\left\{\frac{dC_T}{d(r_0/R)}\right\}_{\text{true}}=\cos^2\phi_0\left\{\frac{dC_T}{d(r_0/R)}\right\}_{v_{to}=0} \tag{A-6}$$

Eq. (A-6) with *Eq.* (A-2) results in

$$\left\{\frac{dC_T}{d(r_0/R)}\right\}_{\text{true}} = \cos^2\phi_0 \frac{\pi}{8}\frac{r_0}{R}\frac{\Delta h}{\rho n^2 R^2} \tag{A-7}$$

(Received May 16, 1968)